Influence of Stator Yoke Thickness and Stator Teeth Shape upon Ripple and Average Torque of Switched Reluctance Motors

Emmanuel Hoang, Bernard Multon, Rafael Vives Fos, Marc Geoffroy

SPEEDAM, 8-10 June 1994, Taormina (Italy), pp.145-149

Influence of Stator Yoke Thickness and Stator Teeth Shape upon Ripple and Average Torque of Switched Reluctance Motors

E. HOANG, B. MULTON, R. VIVES FOS, M. GEOFFROY
L.E.SI.R- U.R.A. C.N.R.S D1375-E.N.S Cachan
61 av du Pdt Wilson 94235 Cachan cedex France
Tel : 33.1.47.40.21.11 Fax : 33.1.47.40.21.99

ABSTRACT

During the investigation of the Switched Reluctance Motor (SRM), we became interested in two apparently secondary parameters which are:

- the thickness of the stator yoke;

- the shape of stator teeth.

In keeping the other geometrical parameters, like the outer and air gap diameters, constant, we could study the impacts from varying these two parameters with respect to:

- the curve of instantaneous single-phase torque;

- the poly-phase ripple torque at low speed with a current supply mode;

- the power semi-conductor rating at maximum power;

- and the size power ratio of the converter with a full-wave voltage supply mode.

A prototype has been built and enables drawing a comparison between the theoretical and practical results.

Keywords : variable reluctance motor, yoke thickness, average torque, ripple torque, converter rating

SPEEDAM, 8-10 June 1994, Taormina (Italy), pp.145-149

I.Introduction

To design a motor meeting specifications, both experience and the use of equations are necessary. These equations take geometrical parameters and some constraints like copper losses into account [2]. An initial geometrical result motivated us to define all parameters, such as outer diameter, pole shaping and air gap radius. However, in order to assess precisely the ratio of average torque per copper losses and to fill coil space in the most optimal way, we became interested in two particular geometrical parameters for the switched reluctance motor (SRM): stator yoke thickness and shape of stator teeth (see Fig. 1).

The use of a 2-D. finite-element software is essential for taking equations which are not linear into account (for example, saturable magnetic material) and for calculating the characteristic variables of a motor, like magnetic flux or torque.

With this software, we can plot :

- In the flux-current set of curves, two extreme position curves (opposition and conjunction) define average torque in the case of an ideal current supply mode.

- Curve network flux in terms of electrical angle for several currents, which helps to estimate the influence of the stator yoke thickness and the shape of stator teeth by means of a simulation software on power semi-conductor rating at maximum power use and on " size power ratio " of the converter. Switched reluctance motor mode with full-wave voltage is also studied. At higher speed, many authors have shown that this supply mode is very efficient.

- Curve network torque in terms of electrical angle for several currents to calculate ripple torque at low running speed .

II.Presentation of motors under study

A.Geometrical definition

In order to optimize several constraints which will be indicated, we modified the stator yoke thickness and the stator tooth shape of a SRM with 6 and 8 teeth at the stator and rotor, respectively a rated speed of 3000 rpm and a rated torque of 9.5 Nm; thus a power of 2.95 kW. The results of a initial sizing provides the dimensions of the machine (Ec1as1) as follows:

- Outer diameter : 143 mm
- Air gap diameter : 82 mm
- Iron active length 80 mm
- $\beta s = 0.32$; $\beta r = 0.48$
- Stator yoke thickness (Ec1) 6.5 mm
- The tooth of the stator and rotor are right-pole shaped.

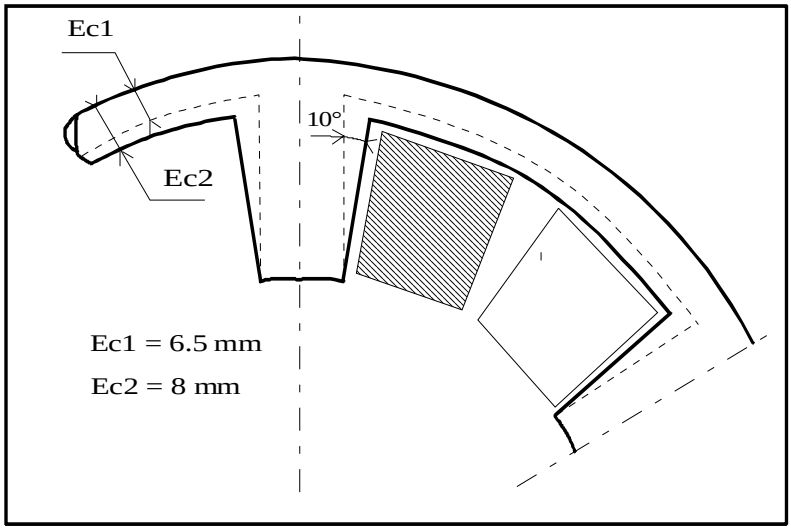

Fig. 1 Stator size of studied machines

B.Magnetic core modifications

The second (Ec2as1) differs from the first in yoke thickness (Ec2 = 8 mm).
The third (Ec2as2) differs from the first in yoke thickness (Ec2 = 8 mm) and in stator pole shape (angle of teeth side = 10°).
The prototype has been built with Ec2as2 geometrical parametric results.

C.Number of spires, winding area

The converter topology is an asymmetric half-bridge per phase and the DC voltage supply is 300 volts. These 300 V are fixed by the power network. To optimise the motor's performance we varied the turn coils. We computed the turns coils to obtain an average torque of 9.5 Nm at 3000 rpm with a DC. supply voltage of 300 V (see section V high speed and voltage feeding).
To compute iron losses :

$$p_{cu} = q\, R\, I_{rms}^{2}$$

$$R = \rho \frac{n\, L}{S_{cu}}$$

n = number of turns, L = average length of a turn

$$L = 2\left(L_a + k_{tb}\left(w_s + \frac{\overline{w_s}}{2} \right) \right)$$

k_{tb} is a coefficient to take into account winding-heads form $\left(1 < k_{tb} < \frac{\pi}{2} k_{tb} \approx 1.3 \right)$.

$$w_s = \frac{2\pi R_e \beta_s}{N_s} \text{ and } \overline{w_s} = \frac{2\pi R_e (1-\beta_s)}{N_s}$$

$$S_{cu} = k_b \frac{S_{bob}}{n}$$

Two methods to compute winding area are:
1 Winding area is equal to the total unoccupied space between stator teeth, and k_b is dependent on coil winding technique.

2 Winding area is a square-shaped and kb is only dependent on coil winding technique and is independent of stator yoke shape.

$S_{bob} = \frac{1}{2}\overline{w_s}\, h_s$ and $k_b \approx 0.6$

h_s = height of stator tooth

machine	Ec1as1	Ec2as1	Ec2as2
Sbob1(m^2)	4.97E-04	4.57E-04	4.14E-04
Sbob2 (m^2)	3.50E-04	3.27E-04	3.27E-04
L (m)	0.234	0.234	0.234
spire number	190	200	187
R1 (Ω)	0.567	0.683	0.659
R2 (Ω)	0.805	0.954	0.834

Table 1.Data on coil realization

III.Presentation of analysis criteria

To compare the machines under study, we have defined analysis criteria:

A.Converter, size power ratio

[5] defines a "sizing factor" which, based on actuator performances (load power, phase voltage and current) and converter topology, allows comparing silicium power.

For one phase : (size power ratio)

$\delta' = \frac{U_{max} I_{rms}}{P_1}$ with P_1 power per phase

$\delta'' = \frac{U_{max} I_{max}}{P_1}$ with P_1 power per phase

For a converter :

$F_d' = n_i \frac{U_{max} I_{rms}}{P}$ with n_i the number of power switches

$F_d'' = n_i \frac{U_{max} I_{max}}{P}$

Example : for AC. motor drive supplied with a PWM voltage, $F_d'' = \frac{8}{\cos\varphi}$

B.Motor performance

B.1 average torque

Average torque is a fundamental piece of data. Four methods are possible to compute average torque.

1 Based on magnetisation curves (Flux-current locus) both in opposition and in conjunction [1](see Fig. 2).

2 Based on data on permeance function $P(\theta)$ and values of Lo, Lc and ls (minimum, maximum and saturated inductance) computiation of converter-machine electromagnetic behaviour [6].

3 With an E.F. 2-D software (Maxwell Ansoft), we can compute the values for several data like poly-phase instantaneous torque, phase current and flux density in different parts of the machine. But computing time is significant (around 100 hours for one operating point).

4 With a E.F. 2-D software (Maxwell Ansoft), we can compute $\text{flux}(\theta, i)$ et $\text{torque}(\theta, i)$ and the simple phase instantaneous torque [7].

computing method :

$$U(t) \rightarrow \frac{d\varphi}{dt} \rightarrow \varphi_n(\theta) = \varphi_{n-1}(\theta) + \frac{d\varphi}{d\theta}$$

$$\varphi(\theta, i) \rightarrow i(\theta)$$

$$\Gamma(\theta, i) \rightarrow \Gamma(\theta)$$

To compare the three machines, we have fixed the average torque at 9.5 Nm.

B.2 Torque ripple

It is difficult to assess the impacts of the torque ripple on noise and on vibration; however, we can define a relative torque ripple by:

$$\Delta\Gamma\,\% = \frac{\Gamma_{max} - \Gamma_{min}}{<\Gamma>}$$

A frequency spectra analysis is useful to have some information on torque ripple harmonics.
This data can be computed accurately in the case of method 3 (computing with E.F. 2-D software).

B.3 Copper losses

(see section II.c *Number of spires, winding area*)

B.4 Iron losses

The loss model utilized takes into account the variation of flux density and we adopt the following formulation :

$p_f\ (W/m^3) = p_h + p_{ec}$

where p_h represents the hysteresis loss component and p_{ec} the eddy current loss component.

$p_h = w_h\, f$ and $w_h = k_{h1}\, \Delta Bpp + k_{h2}\, \Delta Bpp^2$

However, when an induction waveform contains minor loops, an empirical correction must be applied [10]:

$$w_h = (k_{h1}\Delta Bpp + k_{h2}\Delta Bpp^2)\left(1 + \frac{0.32}{\Delta Bpp}\sum_{i=1}^{n}\Delta Bi\right)$$

$$p_{ec} = \frac{1}{T}\int_0^T \alpha_p \left(\frac{dB}{dt}\right)^2 dt$$

with ΔBpp : total variation of flux density.

ΔBi : variation of flux density for minor cycle.

$$\alpha p \approx 1.3\left(\frac{ep^2}{12\rho}\right)$$

ep : steel thickness (mm) ; ρ : resistivity (Ω.m)
for example :
steel : 0.35 mm ;2.8w/$_{kg}$ (1.5T, 50 Hz)
k_{h1}= 5 ; k_{h2} = 40 ; α_p = 0.025

B(t) = sinusoidal waveform. $B(t) \in [-Bm; +Bm]$

$$P_f = \left[kh_1(2B_m) + kh_2(2B_m)^2\right]f + 2\pi^2\alpha_p B_m{}^2 f^2$$

B(t) = triangular waveform. $B(t) \in [0; +Bm]$

$$P_f = \left[kh_1(B_m) + kh_2(B_m)^2\right]f + 4\alpha_p B_m{}^2 f^2$$

When induction is rotational, losses pre-determination is difficult because no rigorous physical model has been developed. Therefore, loss value is usually computed from the loss deduced separately for each of the two orthogonal alternating flux density components [8][9].

Determination of flux density components with E.F. 2D software in different parts of the machines (18 for the rotor, 12 stator teeth and 3 for stator yoke) coupled with the iron loss model allows us to estimate iron loss values.

VI. Low speed and square- wave current supply

A.Ampere turns and copper losses

At low speed, the machine is supplied by square-wave current supply (PWM control), and we have chosen to maximise average torque on copper loss ratio. In Fig. 2 we show energy strokes which have the same area (same average torque of 9.5 Nm). Principals results are presented in Table 2.

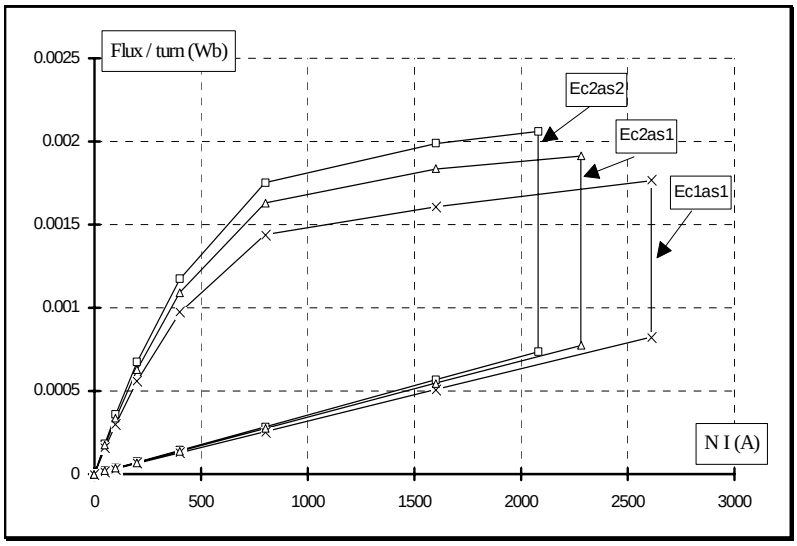

Fig. 2 Magnetization curves

	Ec1as1	Ec2as1	Ec2as2
ampere turns	2609	2280	2080
Irms	9.71	8.06	7.87
Copper losses 1	160	133	122
Copper losses 2	228	186	155
$\frac{\text{average torque}}{R_1 I^2}$	0.0593	0.0714	0.0777
$\frac{\text{average torque}}{R_2 I^2}$	0.0417	0.0511	0.0614

Table 2 Data on copper losses at low speed

We can note that for the same amount converted energy, the increase in yoke thickness and the evolution in the shape of stator teeth allow reducing copper losses at a ratio of 1.22 between Ec1as1 and Ec2as1 machines and at a ratio of 1.2 between Ec2as1 and Ec2as2 machines.

B. Instantaneous torque and ripple torque

With data on single-phase torque at constant current $\text{torque}(\theta, i)$ (see Fig. 3), a simulation allows us to define ripple torque at low speed for a current supply mode.

The square-form ampere turns are 1200, 2400 and 4000 A with 120° angular duration ($\theta on = 15°$; $\theta off = 135°$).

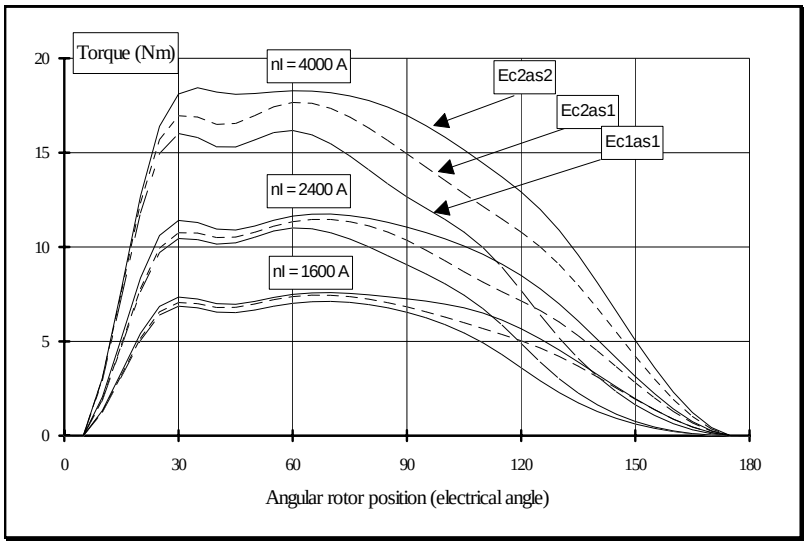

Fig. 3 Instantaneous torque

	N I (A)	Ec1as1	Ec2as1	Ec2as2
average (Nm)	1200	5.63	6.20	6.55
ripple (%)		96%	69%	65%
average (Nm)	2400	8.29	9.34	10.05
ripple (%)		106%	71%	65%
average (Nm)	4000	12.29	14.22	15.68
ripple (%)		98%	71%	68%

Table 3 Data on torque at low speed

We can note that for the same ampere turns, the increase in yoke thickness and the evolution in the shape of stator teeth allow increasing average torque with a lower relative torque ripple.

With a current feeding to minimise the torque ripple [7], single phase instantaneous torque of the Ec2as2 machine permits obtaining a lower torque ripple on a wider speed range.

V.High speed and voltage feeding

To maximise the converter's silicium power at high speed, it is necessary to feed SRM with a square-wave voltage . We sought to obtain the same average torque (9.5 Nm) at the same speed (3000 rpm, electric frequency = 400 Hz) and at a DC voltage supply of 300 V by optimising turn coils and control parameters (ψ = advance angle relative to unaligned inductance and θp = electrical magnetisation, $\theta p = \theta off - \theta on$, $\psi = -\theta on$).

Control angles are the same for the three machines (ψ = 70° electrical angle and θp = 180° electrical angle, see section II.c for number of turns).

In Fig. 4 to Fig. 7, elements of comparison are presented.

In Fig. 4 current phases are represented, in Fig. 5 the magnetization curves in the case of voltage fed, in Fig. 6 it's the poly-phase instantaneous torque.

In Fig. 7 relative ripple torque spectra analyses are represented. The first harmonic is q.f = 3*400 Hz.

Principals results are presented in Table 4.

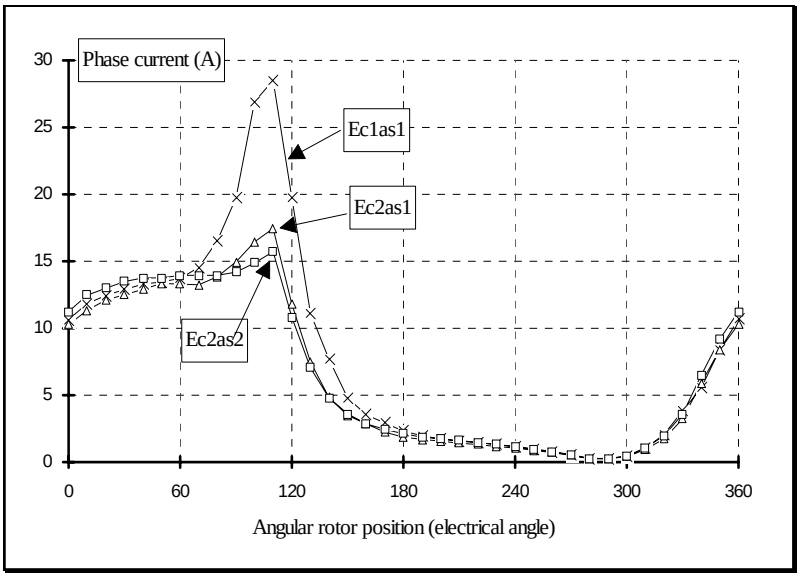

Fig. 4 Current phase

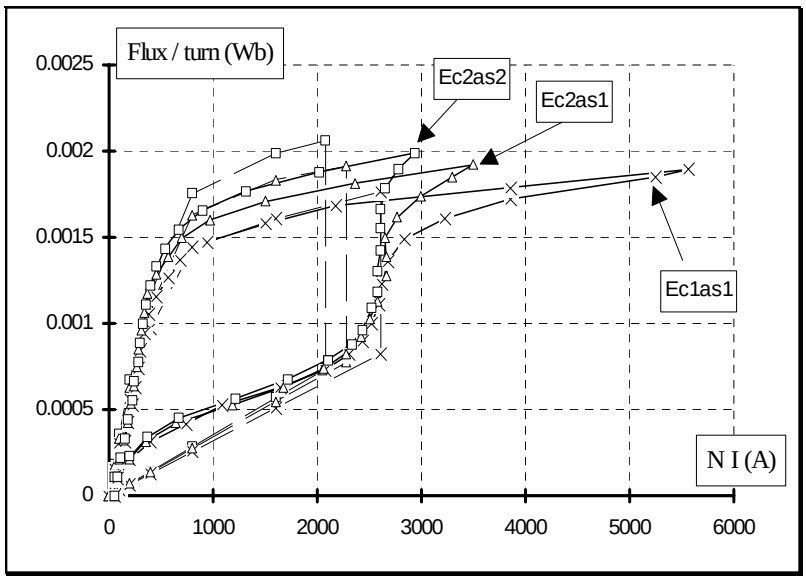

Fig. 5 Magnetization curves on voltage fed

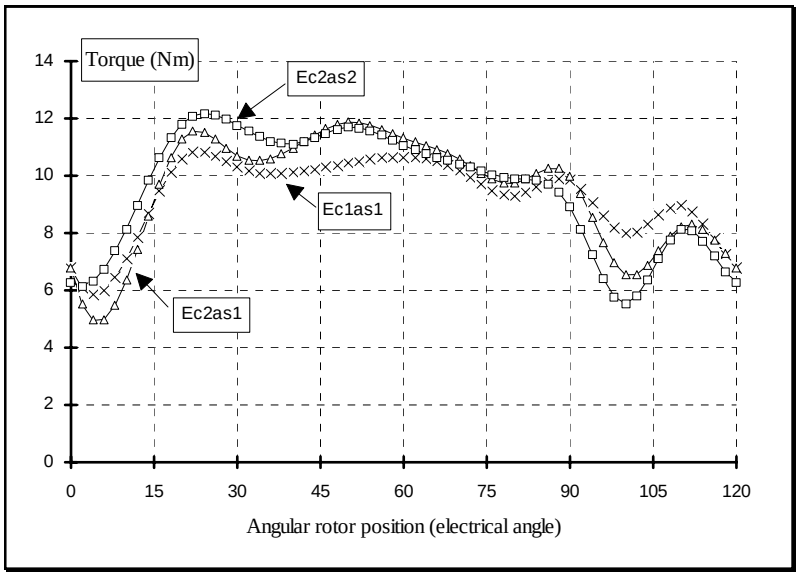

Fig. 6 Poly-phase instantaneous torque

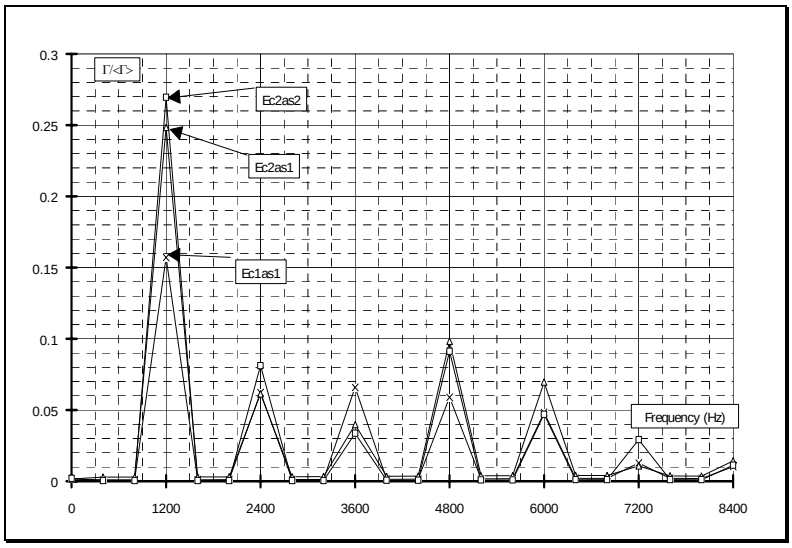

Fig. 7 Ripple torque spectra

	Ec1as1	Ec2as1	Ec2as2
Pu (W)	2917	2966	2987
<Γ> (Nm)	**9.29**	**9.44**	**9.51**
ΔΓ (Nm)	4.84	5.95	6.27
ΔΓ (%)	52%	63%	66%
Γ1/<Γ>	0.16	0.25	0.27
copper losses (W)	**354**	**210**	**188**
Irms (A)	12.11	8.56	8.66
Imax(A)	28.51	17.5	15.72
Fd' (V A/W)	**7.5**	**5.2**	**5.2**
Fd" (V A/W)	**17.6**	**10.5**	**9.5**
Iron losses (W)	**115**	**94**	**101**
rotor (W)	44.6	39.7	39.9
stator (W)	70.7	53.7	61.0
efficiency	**86.1 %**	**90.7 %**	**91.1 %**

Table 4 Data on studied machines at high speed

The increase in yoke thickness and the evolution in the shape of stator teeth, with voltage fed, and at a same level of average torque, allow reducing copper losses, the size power ratio and increasing the efficiency. However iron losses and ripple torque increase between Ec2as1 and Ec2as2 machines.

A complementary study of a machine with a yoke thickness equal to 9.5 mm permits to reduce iron losses of 10 % but the copper increase. The efficiency increase from 91.1 % to 91.4 %.

VI.Conclusion

It is possible to find optimal stator geometrical parameters taking analysis criteria into account, such as, ripple torque at low speed, power semi-conductor rating at maximum power and "size power ratio" of the converter at high speed in full-wave voltage supply mode. Optimal stator yoke thickness value increases with the average torque level; however, there is a limit to this value at oversaturation of the magnetic material. For the second parameter under study, it is worthwhile to make stator teeth with a trapezoidal shape in order to improve the instantaneous torque diagram and thereby to reduce ripple torque.

VII.Nomemclature

Ec	:	stator yoke thickness
n	:	number of turn coil for one phase
L	:	average length of one turn coil
La	:	iron active length
βs	:	reduce stator pole arc
βr	:	reduce rotor pole arc
Re	:	air gap radius
Ns	:	number of stator teeth
S_{bob}	:	winding area
S_{cu}	:	copper area for one conductor
U_{max}	:	maximal voltage for one phase
I_{max}	:	maximal current for one phase
I_{rms}	:	RMS current for one phase
P_1	:	active power for one phase
P	:	total active power
$<\Gamma>$	:	average torque
Γ_{max}	:	maximal poly-phase torque
Γ_{min}	:	minimal poly-phase torque
Γ_1	:	amplitude of the first torque harmonic

VIII.References

[1] **P.J Lawrenson, J.M Stephenson, P.T. Blenkinsop, J. Corda, N. Fulton**
Variable Speed Switched Reluctance Motors
IEE Proc. B, Elect. Power Appl., vol. 127, pp 253-265, July 1980.

[2] **B. Multon, D. Bonot, J.M. Hube**
Conception d'un Moteur à Réluctance Autocommuté Alimenté en Courant.
MOPP Lausanne, pp. 215-226, Juillet 1990.

[3] **J.V. Byrne, M.F. McMullin**
Design of a Reluctance Motor as a 10 kW Spindle Drives.
MOTORCON (Genève). Sept. 1982. pp. 10-24.

[4] **A.R. Eastham, H Yuan, G.E. Dawson, P.C. Choudhury, P.M.Cusack**
A Finite Element Evaluation of Pole Shaping in Switched Reluctance Motors
Electrosoft 1990. Vol. n°1, pp. 55-67.

[5] **B. Multon, C. Glaize**
Size Power Ratio Optimization for The Converters of Switched Reluctance Motors
IMACS TC1'90, Nancy, pp. 325-331, 19-21 Sept. 90.

[6] **S. Hassine**
Optimisation des Paramètres de Commande en Tension des Machines à Réluctance Variable Autopilotées en Régime Permanent
Thèse de doctorat es sciences. Paris XI. E.N.S. Cachan , 30 Janvier 1992.

[7] **J. Y. Lechenadec, B. Multon, S. Hassine**
Current Feeding of Switched Reluctance Motor. Optimization of the the current Waveform to Minimize the Torque Ripple.
IMACS TC1'93, Montréal, pp. 267-272, 7-9 July 1993

[8] **T. Yamaguchi, K. Narita**
Rotational Power Losses in Commercial Silicon-Iron Laminations
Elec. Eng. in Japan, vol 96, no. 4, pp 15-20, 1976.

[9] **K. Atallah, Z. Q. Zhu, D. Howe**
An Improved Method for Predicting Iron Losses in Brushless Permanent Magnet DC Drives
IEEE Trans. Magn., vol 28, no. 5, pp 2997-2999, 1992.

[10] **J.D. Lavers, P.P. Biringer, H. Hollitscher**
A Simple Method of Estimating the Minor Loop Hysteresis Loss in Thin Laminations
IEEE Trans. Magn., vol 14, pp 386-388, 1978.